SUPPLEMENTARY INFORMATION

8 Tables and 6 Figures

How Much Backbone Motion in Ubiquitin is Really Required to be Consistent with Dipolar Coupling Data Measured in Multiple Alignment Media as Assessed by Independent Cross-Validation?

G. Marius Clore*,† and Charles D. Schwieters*,§

†Laboratory of Chemical Physics, Building 5, National Institute of Diabetes and Digestive and Kidney Diseases, National Institutes of Health, Bethesda, MD 20892-0520, U.S.A.

§Division of Computational Bioscience, Building 12A, Center for Information Technology, National Institutes of Health, Bethesda, MD 20892-5624, U.S.A.

Table 1S Alignment media

Medium Number	Medium composition	Reference
1	CHAPSO/DLPC/CTAB (10:50:1) 5%	(1,2)
2	CHAPSO/DLPC/SDS (10:50:1) 5%	(1,2)
3	Purple membrane fragments (2 mg/ml, 100 mM NaCl)	(1,2)
4	Phage pf1 5 mg/ml 50 mM NaCl	(1,2)
5	Helfrich phases (cetylpyridinumbromide/hexanol = 1:1.33, 25 mM NaBr, 5%)	(1,2)
6	CHAPSO/DLPC (1:5) 5%	(1,2)
7	CHAPSO/DLPC/CTAB (10:50:1) 4%	(1,2)
8	n-dodecyl penta(ethylene glycol)/n-hexanol (r=0.96)	(1,2)
9	polyacrylamide gel (7%)	(1,2)
10	DMPC/DHPC (3:1) 5%	(3)
11	DMPC/DHPC/CTAB (3:10:1) (5%)	(3)

(1) Peti, W.; Meiler, J.; Brüschweiler, R.; Griesinger, C. *J. Am. Chem. Soc.* 2002, *124*, 5822-5833.

(2) Hus, J. -C.; Peti, W., Griesinger, C.; Brüschweiler, R. *J. Am. Chem. Soc.* **2003**, *125*, 5596-5597.

(3) Cornilescu, G.; Marquardt, J. L.; Ottiger, M.; Bax, A. *J. Am. Chem. Soc.* **1998**, *120*, 6836-6837.

Table 2S Pairwise normalized scalar products of alignment tensors for ubiquitin in the 11 media.[a]

Medium	1	2	3	4	5	6	7	8	9	10	11
1	1.00	0.952	-0.873	0.626	0.925	0.730	0.931	0.845	0.855	0.634	0.894
2		1.00	-0.898	0.681	0.847	0.733	0.883	0.733	0.870	0.642	0.848
3			1.00	-0.864	-0.824	-0.391	-0.655	-0.540	-0.622	-0.266	-0.590
4				1.00	0.731	0.123	0.387	0.273	0.413	0.018	0.308
5					1.00	0.558	0.823	0.711	0.716	0.466	0.722
6						1.00	0.921	0.879	0.952	0.990	0.949
7							1.00	0.935	0.956	0.816	0.996
8								1.00	0.904	0.828	0.940
9									1.00	0.910	0.959
10										1.00	0.905
11											1.00

[a]The alignment tensors were obtained by SVD analysis using the coordinates of the NMR structure 1D3Z.

Table 3S Summary of the refinement calculations for ensemble size $N_e = 2$.[a]

	Width of piecewise quadratic potential[b]		
	2r	2pr	2u
relative atomic positions	0.5 Å	1.0 Å	term off
D_a^{NH}	0[c]	10%[b]	10%[b]
rhombicity	0[c]	0.15	0.15

[a]The 3 sets of structures summarized in the table represent the most restricted case (2r), a partially restricted case (2pr), and the least restricted case (2u). However, a number of additional calculations were carried out. These included the following combinations of widths for the relative atomic positions, D_a^{NH} and rhombicity, respectively: 0.5 Å, 5% and 0.075; 0.5 Å, 10% and 0.15; 1.0 Å, 0% and 0; 1.0 Å, 5% and 0.075. The results of these calculations are very similar to those for the 2r and 2pr calculations. The calculations were repeated multiple times using different random number seeds for the assignment of initial velocities, resulting in a total of 100 ensembles for each set of calculations.

[b]The total widths of the flat portion of the piecewise quadratic potential (general formula given by Eq. 6, main text) are $2\Delta l_{RAP}$ for the relative atomic positions term, $2\Delta D_a$ for D_a, and $2\Delta\eta$ for the rhombicity η. In the case of D_a, the widths in the table are expressed as a percentage of D_a (since the absolute value of D_a varies over a large range for the 11 different media).

[c]A width of zero indicates that the potential term is represented by a simple harmonic oscillator.

Table 4S Dipolar coupling R-factors

	Dipolar coupling R-factor (%)[a]					
	X-ray	NMR[b]	Refined structures[c]			
	(1UBQ)	(1D3Z)	n=1	n=2(r)	n=2(pr)	n=2(u)
NH dipolar couplings[d]						
medium 1 (62)	14.2	11.9	3.9±0.1	3.5±0.1	3.1±0.2	3.0±0.2
medium 2 (55)	25.3	21.1	10.5±0.2	8.4±0.6	7.4±0.7	6.9±0.8
medium 3 (60)	22.8	18.5	9.1±0.2	6.7±0.3	6.1±0.4	5.9±0.5
medium 4 (48)	18.7	16.4	8.5±0.2	6.3±0.6	5.6±0.7	5.0±0.7
medium 5 (55)	17.5	14.0	4.4±0.2	3.9±0.3	3.6±0.3	3.5±0.3
medium 6 (54)	14.8	11.4	11.9±1.9	12.2±1.7	12.9±2.3	12.5±2.3
medium 7 (48)	13.6	10.8	6.7±0.2	6.1±0.2	5.7±0.3	5.8±0.5
medium 8 (65)	15.2	13.3	13.3±0.9	13.3±1.2	13.2±1.6	12.8±1.4
medium 9 (56)	35.6	17.4	23.7±7.3	19.5±4.3	22.9±7.0	22.4±6.7
medium 10 (63)	12.5	5.3[b]	5.4±0.4	4.9±0.3	4.9±0.4	5.0±0.4
medium 11 (65)	10.7	6.4	5.8±0.2	3.5±0.1	3.3±0.2	3.4±0.2
N-C' dipolar couplings[d]						
medium 10 (61)	13.0	6.4[b]	8.9±0.5	9.1±0.4	9.0±0.5	9.1±0.6
medium 11 (63)	12.3	7.3[b]	7.7±0.4	7.1±0.5	7.1±0.6	7.0±0.6
HN-C' dipolar couplings[d]						
medium 10 (61)	15.6	8.8[b]	10.3±0.4	9.9±0.3	9.4±0.5	9.4±0.4
medium 11 (63)	17.1	11.0[b]	12.0±0.3	11.2±0.3	10.9±0.3	10.9±0.6
Cα-C' dipolar couplings[d]						
medium 10 (58)	9.5	7.1[b]	7.4±0.4	6.9±0.3	7.1±0.6	7.1±0.4
medium 11 (54)	14.5	8.2[b]	8.2±0.5	7.2±0.4	7.5±0.4	7.5±0.4
Cα-Hα dipolar couplings[d]						
medium 10 (62)	17.0	6.3[b]	15.6±0.8[c]	13.6±0.7[c]	13.7±0.8[c]	13.3±1.1[c]
medium 11 (62)	16.4	4.8[b]	14.0±1.0[c]	11.8±0.7[c]	12.1±1.0[c]	11.7±1.2[c]
H_N-Hα dipolar couplings[d]						
medium 10 (65)	19.9	17.2	19.5±0.7[c]	19.1±0.7[c]	18.9±0.8[c]	19.0±0.7[c]

Footnotes to Table 4S

[a]The dipolar coupling R-factor is given by the ratio of the r.m.s. difference between observed and calculated values and the expected value of the r.m.s. difference if the vectors were randomly oriented. The latter is given by $[2D_a(4 + 3\eta^2)/5]^{1/2}$.[15] For the ^1H-^1H dipolar couplings, the distance between the protons isn't fixed. Consequently, the denominator is given by $\{2<D_{obs}^2>\}^{1/2}$.

[b]The NMR structure 1D3Z is the result of cartesian coordinate refinement against all the dipolar couplings measured in media 10 and 11, with the exception of the NH dipolar coupling in medium 11 and the H_N-Hα dipolar couplings in medium 10 which were not included in the structure determination.

[c]The refined structures were refined against all dipolar couplings with the exception of the Cα-Hα dipolar couplings in media 10 and 11, and the H_N-Hα dipolar couplings in medium 10. Since the Cα-Hα vector and the N-H vectors are independent of each other, and since the Cα-Hα dipolar coupling data are of high quality, the cross-validated (free) Cα-Hα dipolar coupling R-factors provide a reliable means of assessing whether the improvement in agreement against the fitted dipolar couplings upon increasing the ensemble size is significant or simply a consequence of over-fitting. In each case, the values and standard deviations reported are obtained by averaging over all 100 calculated ensembles.

[d]The number of experimental dipolar couplings are listed in parentheses.

Table 5S D_a^{NH} and rhombicity for the different alignment tensors

	Da^{NH} (Hz)/rhombicity[a]					
	X-ray (1UBQ)	NMR (1D3Z)	Refined structures n=1	n=2(r)	n=2(pr)	n=2(u)
medium 1	28.5 0.36	28.4 0.32	29.2±0.2 0.29±0.01	30.0±0.2 0.29±0.01	30.0±1.3 0.29±0.07	30.4±1.2 0.28±0.07
medium 2	15.8 0.40	16.0 0.39	17.3±0.1 0.38±0.01	18.1±0.3 0.39±0.02	18.1±0.9 0.39±0.08	18.5±0.9 0.38±0.08
medium 3	-16.6 0.00	-17.1 0.05	-18.2±0.1 0.06±0.02	-19.3±0.3 0.09±0.02	-19.7±0.9 0.09±0.07	-20.3±1.1 0.09±0.07
medium 4	12.7 0.42	12.9 0.49	14.1±0.1 0.40±0.01	14.6±0.3 0.43±0.03	15.1±0.7 0.42±0.07	15.7±0.8 0.42±0.07
medium 5	20.9 0.22	20.4 0.25	22.4±0.2 0.22±0.01	22.8±0.4 0.21±0.02	23.0±1.0 0.22±0.07	23.3±0.8 0.22±0.07
medium 6	-5.9 0.22	-5.8 0.21	-5.9±0.1 0.18±0.06	-6.0±0.1 0.21±0.02	-6.0±0.3 0.19±0.06	-6.1±0.4 0.19±0.07
medium 7	-13.8 0.59	-13.4 0.61	-13.4±0.1 0.64±0.07	-13.7±0.2 0.63±0.01	-13.7±0.5 0.63±0.03	-13.8±0.5 0.63±0.03
medium 8	-7.3 0.30	-7.1 0.30	-7.0±0.1 0.29±0.02	-7.3±0.1 0.28±0.02	-7.4±0.4 0.27±0.07	-7.4±0.4 0.28±0.07
medium 9	2.4 0.38	-2.5 0.65	-2.6±0.1 0.47±0.10	-2.7±0.1 0.51±0.04	-2.7±0.2 0.50±0.09	-2.7±0.3 0.52±0.09
medium 10	-9.6 0.16	-9.8 0.16	-9.5±0.1 0.16±0.01	-9.8±0.1 0.16±0.01	-9.9±0.4 0.15±0.01	-10.0±0.4 0.15±0.01
medium 11	-15.4 0.49	-15.6 0.50	-15.0±0.1 0.52±0.01	-15.5±0.1 0.52±0.01	-15.6±0.6 0.52±0.06	-15.8±0.7 0.51±0.07
medium 10*[b]	-9.9 0.19	-9.9 0.16	-9.9±0.1 0.15±0.01	-10.1±0.1 0.15±0.01	-10.2±0.4 0.14±0.05	-10.3±0.4 0.14±0.06

Footnotes to Table 5S

[a]The first number listed is D_a^{NH}, and the second is the rhombicity. The values and standard deviations reported are obtained by averaging over all 100 calculated ensembles.

[b]Medium 10* is nominally the same as medium 10 but the measurements ($^1D_{NH}$ and D_{HH}) were carried out on a different sample using a different batch of DMPC/DHPC bicelles. Consequently the values of D_a^{NH} and η are slightly different. The data collected in medium 10* were not included in the refinement calculations.

Table 6S Agreement with NOE-derived interproton distance restraints, ^3J couplings and idealized geometry.

	X-ray (1UBQ)	NMR (1D3Z)	Refined structures $N_e = 1$	$N_e = 2$(r)	$N_e = 2$(pr)	$N_e = 2$(u)
R.m.s from NOE-derived interproton distance restraints (1119)(Å)[a,b]						
$r_{NOE}^{(struct)}$	0.093	0.000	0.004±0	0.003±0.002	0.005±0.002	0.007±0.003
$r_{NOE}^{(ens)}$				0.000±0	0.001±0.001	0.001±0.001
R.m.s. from ^3J couplings (Hz)[a,c]						
$^3J_{HNH\alpha}$ (63)	0.71	0.63	0.69±0.04	0.74±0.03	0.75±0.04	0.78±0.05
$^3J_{HNC\beta}$ (60)	0.31	0.26	0.34±0.01	0.32±0.01	0.33±0.01	0.34±0.01
$^3J_{HNC'}$ (61)	0.46	0.49	0.54±0.02	0.55±0.01	0.57±0.02	0.57±0.02
$^3J_{C'H\alpha}$ (65)	0.29	0.28	0.31±0.01	0.32±0.01	0.33±0.01	0.33±0.01
$^3J_{C'C\beta}$ (57)	0.18	0.14	0.20±0.01	0.20±0.01	0.21±0.01	0.21±0.01
$^3J_{C'C'}$ (56)	0.25	0.21	0.26±0.01	0.24±0.01	0.24±0.01	0.25±0.01
R.m.s. from χ_1 side chain torsion angle restraints (35) (deg)[a,b]	0.10	0	0.28 ±0.34	0.07±0.11	0.09±0.18	0.12±0.23
Deviations from idealized covalent geometry						
bonds (Å)	0.017	0.006	0.004±0	0.004±0	0.004±0	0.004±0
angles (deg.)	3.07	0.81	0.73±0.02	0.75±0.03	0.77±0.02	0.74±0.03
improper torsions (deg.)	3.26	0.68	1.29±0.06	1.30±0.07	1.34±0.01	1.32±0.08

Footnotes to Table 6S

[a]The number of experimental terms are listed in parentheses.

[b]The NOE-derived interproton distance restraints and χ_1 side chain torsion angle restraints are included in the target function used for refinement. There are no NOE violations >0.2 Å or torsion angle violations greater than 5° for either the 1D3Z NMR coordinates or the refined structures. For the X-ray coordinates (1UBQ) there are 10 interproton distance violations greater than 0.5 Å. $r_{NOE}^{(ens)}$ and $r_{NOE}^{(struct)}$ are defined in Eqs. 12 and 13 (in main text), respectively.

[c]The ^3J couplings are *not* included in the target function for refinement and therefore serve as an independent check on the results. Note that the coefficients for the Karplus equations relating ^3J to torsion angles were derived by initially best-fitting to the X-ray (1UBQ) coordinates. For the ensemble size $N_e = 2$ calculations, the reported values represent the ensemble averaged values.

Table 7S Backbone atomic r.m.s. differences

	Ensemble size			
	N_e = 1	N_e = 2(r)	N_e = 2(pr)	N_e = 2(u)
Backbone atomic r.m.s. differences (Å)				
Intra-ensemble				
before best-fitting		0.43±0.07	0.70±0.20	2.33±0.65
after best-fitting		0.42±0.07	0.63±0.20	1.01±0.34
Mean coordinates of each ensemble				
versus overall refined mean	0.17±0.04	0.12±0.02	0.16±0.02	0.16±0.03
versus NMR (1D3Z)	0.52±0.03	0.44±0.03	0.45±0.03	0.40±0.03
versus X-ray (1UBQ)	0.58±0.03	0.53±0.03	0.54±0.03	0.50±0.03
Average intra-ensemble rigid body rotational difference (deg.)		0.3	1.0	7.0

Table 8S ϕ/ψ backbone torsion angles of the three residues (L69, E51 and A28) with the lowest S^2(jump) values, together with those of their sequential neighbors for the members of a typical N_e = 2 ensemble, showing compensatory changes in ϕ/ψ that preserve the path of the polypeptide chain. The ϕ/ψ values relate specifically to the pair of structures from one ensemble from the 2r set of calculations shown in Figs. 7 and 8 of the Main Text. Also listed for comparison are the average values of the inter-structure N-H bond vector angles and S^2(jump) order parameters for the N-H vectors, together with their standard deviations, derived from the 100 calculated ensembles.

Residue	<inter-structure N-H bond vector angles> (deg.)	<S^2(jump)> for N-H bond vectors	ϕ/ψ [a] structure 0	structure 1
T66	6.8±3.7	0.99±0.01	-112/127	-109/131
L67	7.3±3.9	0.98±0.02	-108/143	-108/160
H68	22.0±2.6	0.89±0.02	-104/110	-100/166
L69	74.5±2.0	0.30±0.01	-84/137	-141/110
V70	10.6±3.1	0.97±0.01	-125/136	-116/138
L71	15.3±5.4	0.94±0.04	-76/139	-95/140
Q49	16.9±7.6	0.93±0.06	-79/132	-73/131
L50	21.3±4.5	0.90±0.04	-95/123	-73/164
E51	70.5±2.1	0.33±0.02	-72/163	-134/150
D52	8.6±2.0	0.98±0.01	-76/10	-72/-24
G53	9.7±5.2	0.97±0.03	-100/-4	-98/0
V26	17.1±3.6	0.93±0.02	-68/-51	-64/-38
K27	17.4±3.1	0.93±0.02	-58/-79	-64/-36
A28	47.5±7.2	0.59±0.08	-20/-40	-73/-34
K29	21.7±4.4	0.89±0.04	-66/-42	-64/-38
I30	11.4±2.8	0.97±0.01	-66/-36	-63/-42

[a]All ϕ/ψ angles lie within the most favored region of the Ramachandran map with the exception of those for Lys27 and Ala28 of structure 0 which lie in the additionally allowed region of the map.

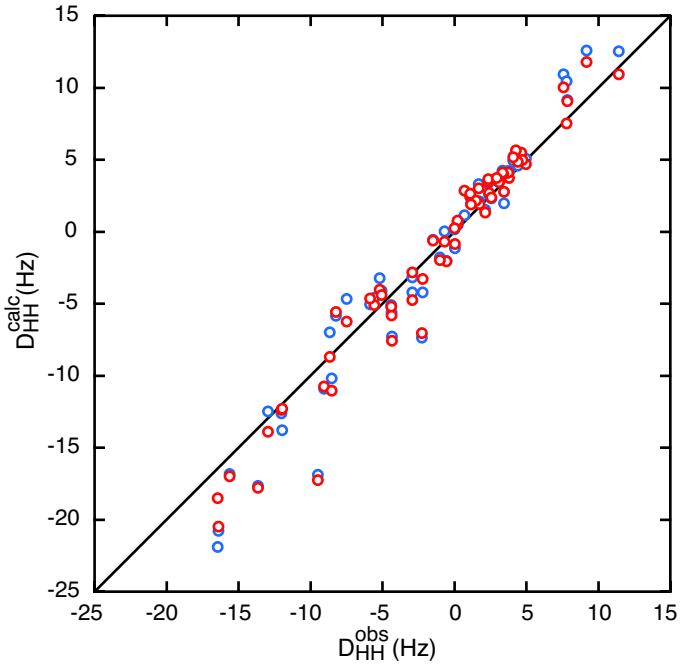

Fig. 1S Correlation plot between observed and calculated ^{1}H-^{1}H dipolar couplings measured in medium 10* (DMPC/DHPC bicelles) for structures refined with ensemble sizes of N_e =1 (blue) and 2 (red). The alignment tensor employed is that obtained by best-fitting the $^{1}D_{NH}$ dipolar coupling data measured in the identical sample to the refined coordinates (see Table 5S, medium 10*). There is no evidence for any deviation from a slope of 1 for the correlation between observed and calculated between H_N-Hα dipolar couplings. This is in direct contrast to a previous report (cf. Fig. 4 of Peti, W.; Meiler, J.; Brüschweiler, R.; Griesinger, C. *J. Am. Chem. Soc.* 2002, *124*, 5822-5833) in which it was claimed that the H_N-Hα vectors experience a larger alignment tensor than the N-H bond vectors, a result which was interpreted as independent evidence for significant degrees of motion for the backbone N-H bond vectors. However, inspection of the correlation plot between observed and calculated $^{1}D_{HH}$ dipolar couplings shown in Peti *et al.* suggests, in retrospect, that the apparent deviation from a slope of 1 represents a fitting artifact as a consequence of the large scatter and poor correlation between observed and calculated values.

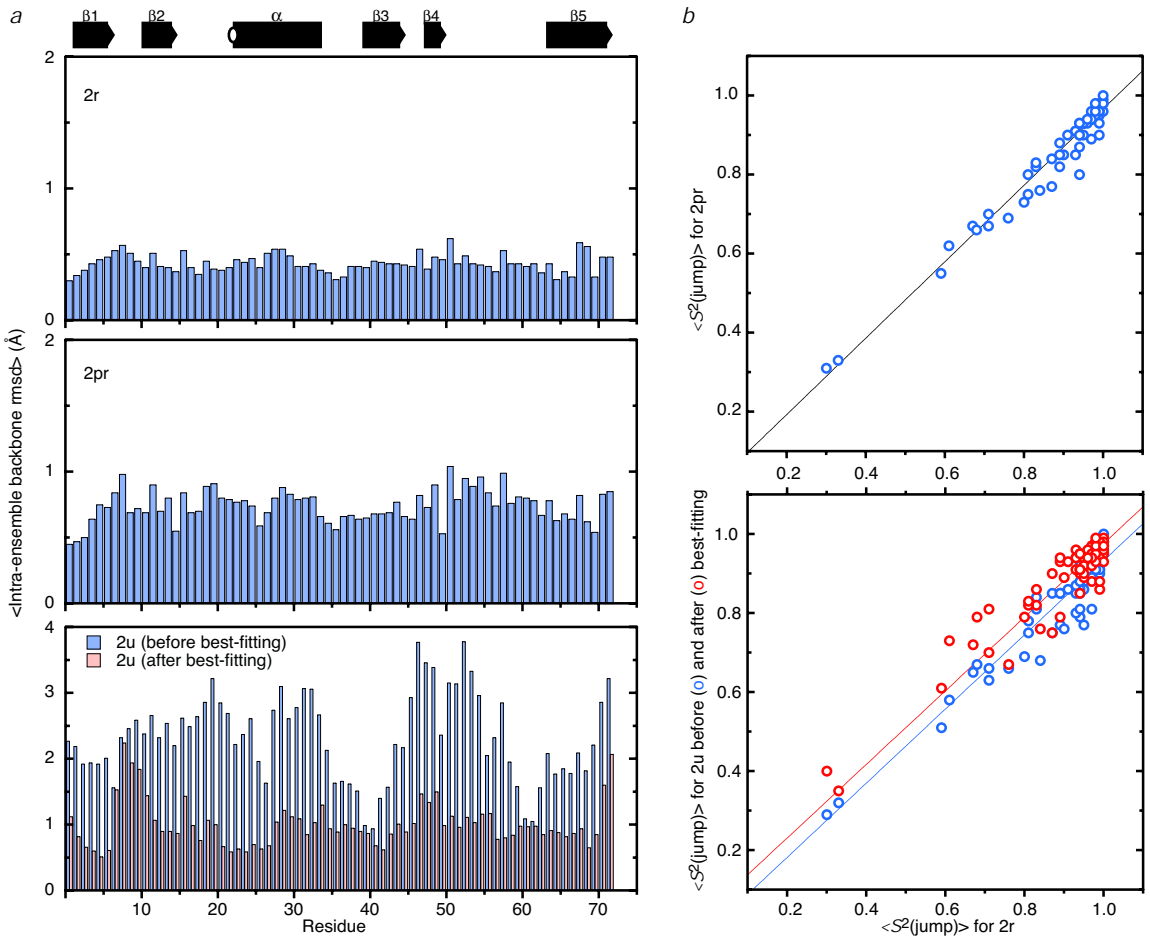

Fig. 2S Comparison of results obtained for an ensemble size $N_e = 2$ from the 2r (restricted), 2pr (partially restricted) and 2u (unrestricted) calculations. (a) Average intra-ensemble backbone (N, Cα, C' atoms) r.m.s. deviation. (b) Correlation between the calculated order parameters $\langle S^2(\text{jump})\rangle$ for the 2r set of structures versus those for the 2pr and 2u set of structures. The angle brackets <> denote averaging over all 100 calculated ensembles. Color code: blue, before rotational best-fitting of the backbone coordinates; red, after rotational best-fitting of the backbone coordinates. Although there is a substantial increase in the intra-ensemble backbone atomic r.m.s. difference between two members of each ensemble on going from the 2r to the 2u set of calculations, the calculated S^2(jump) order parameters for the N-H bond vectors remain very similar for the three set of calculations.

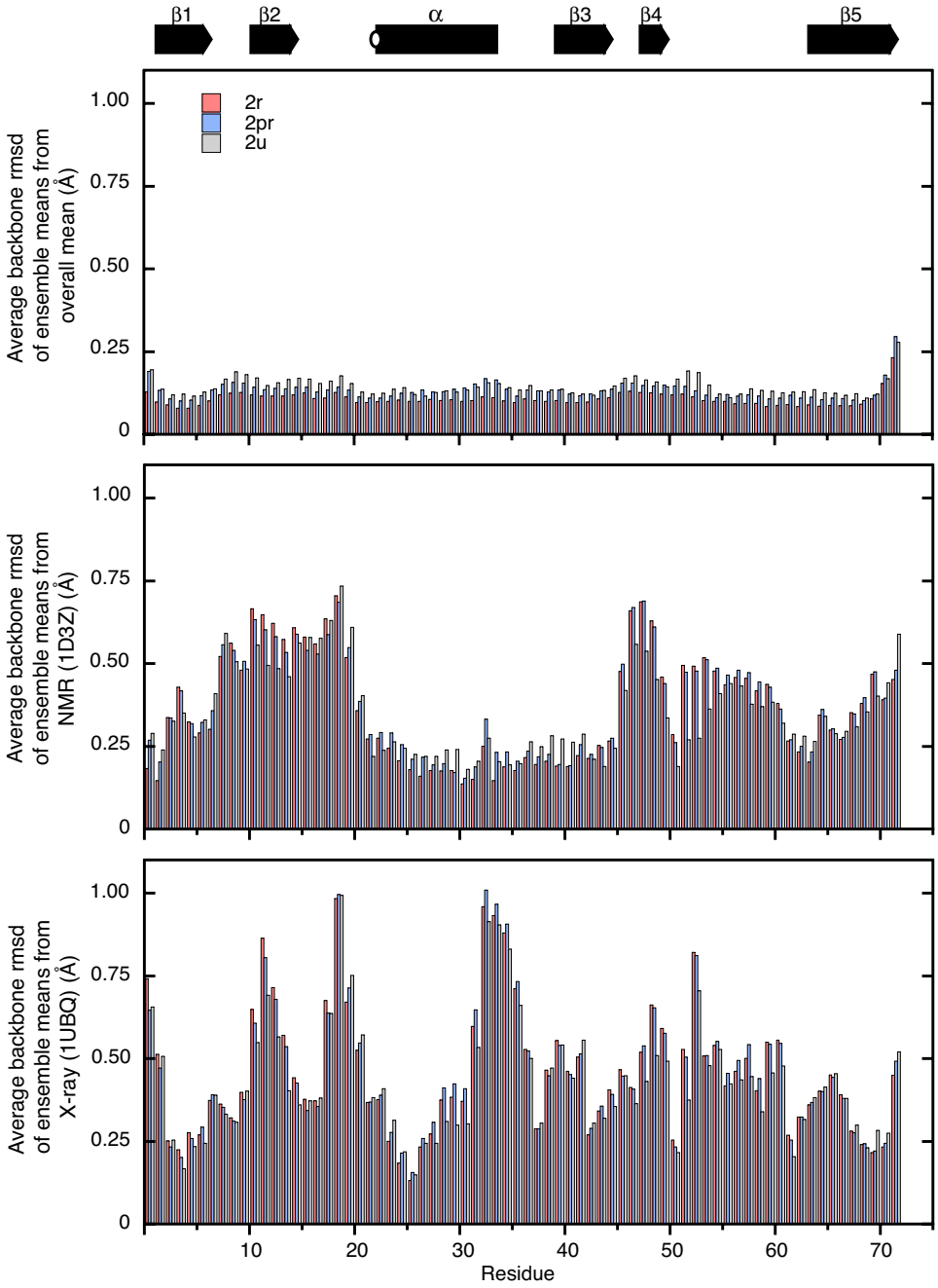

Fig. 3S Comparison of the ensemble $N_e = 2$ structures (2r, 2pr and 2u calculations) with the NMR (1D3Z) and X-ray (1UBQ) coordinates. Color code: 2r, red; 2pr, blue; 2u, grey. The backbone atomic r.m.s. difference between the ensemble means and the corresponding overall mean (averaged over 100 calculated ensembles) is very small (top panel). The overall mean coordinates from the 2r, 2pr and 2u set of calculations are almost identical, as is evident from the comparisons with the NMR (1D3Z) and X-ray coordinates (middle and lower panels, respectively).

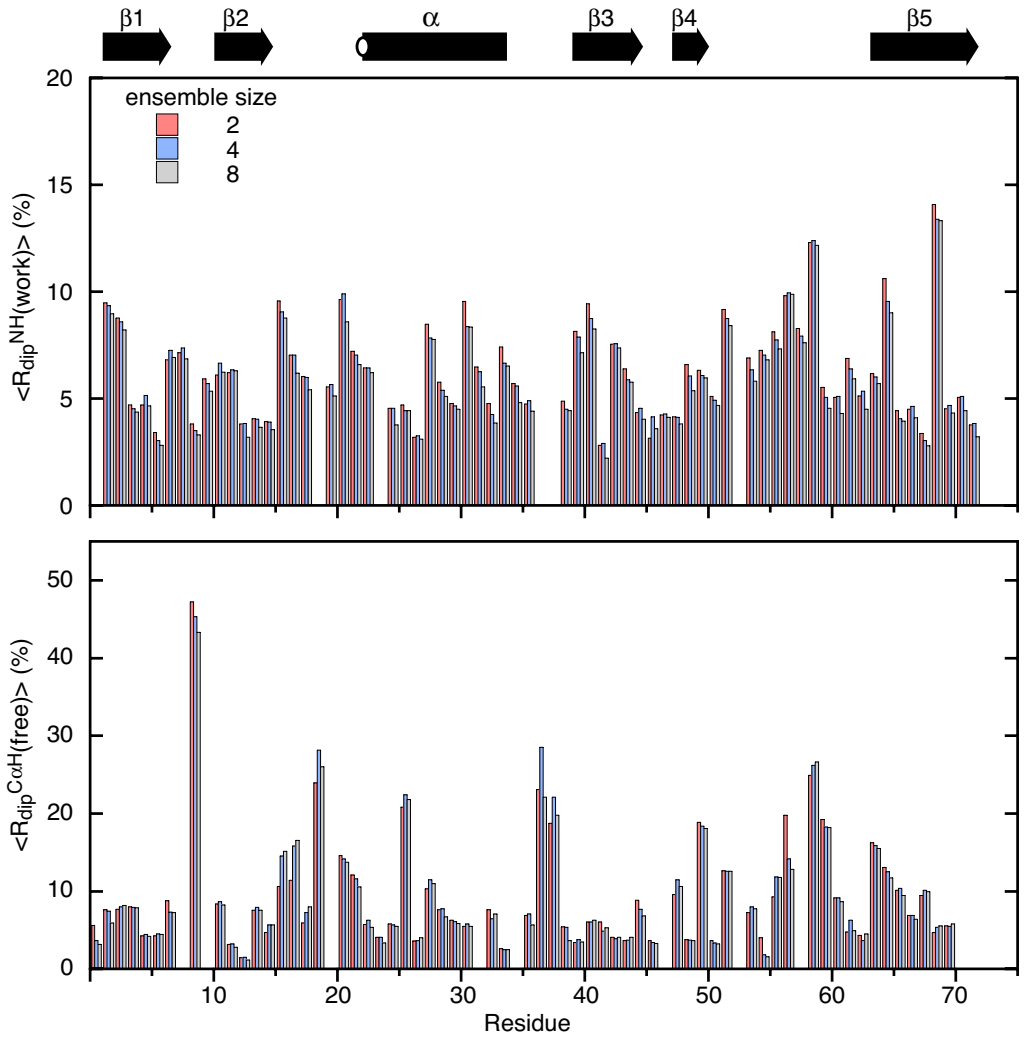

Fig. 4S Effect of increasing the ensemble size (N_e = 2, 4 and 8) on the residue-based working, $\langle R_{dip}^{NH}(work)\rangle$, and cross-validated, $\langle R_{dip}^{C\alpha H}(free)\rangle$, dipolar coupling R-factors averaged over media 1-11 and media 10-11, respectively. (The angle brackets <> denote averaging over all 100 calculated ensembles.) The data presented were obtained using the restricted 2r conditions set out in Table 3S. Similar results were obtained using the partially restricted and unrestricted conditions set out in Table 3S. Color code: N_e = 2, red; N_e = 4, blue; N_e = 8, grey.

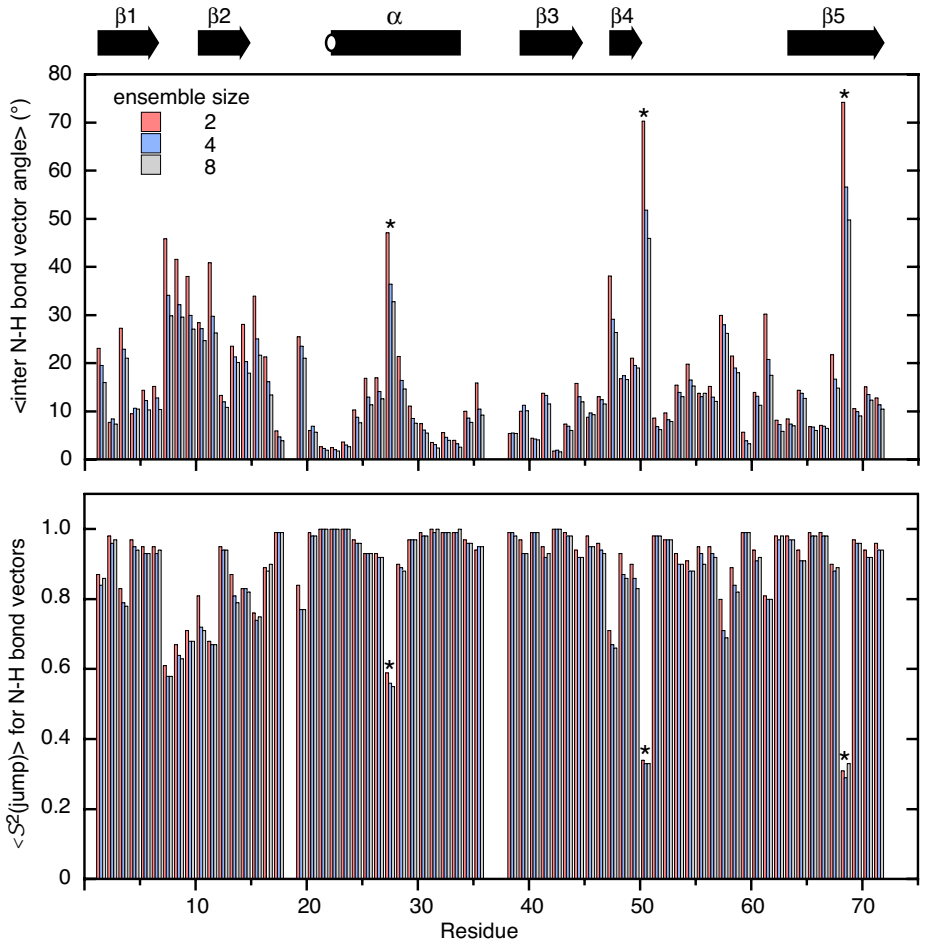

Fig. 5S Effect of increasing the ensemble size (N_e = 2, 4 and 8) on the average inter-structure N-H bond vector angles within an ensemble and corresponding order parameters S^2(jump). The angle brackets <> denote averaging over all 100 calculated ensembles. Color code: N_e = 2, red; N_e = 4, blue; N_e = 8, grey. The asterisks in the figure denote the three residues, A28, E51 and K69 with especially large anisotropic N-H bond vector motions. As discussed in the main text, the magnitude of these motions may be overestimated as a consequence of possible errors in the measured $^1D_{NH}$ dipolar coupling data for these residues in a few media.

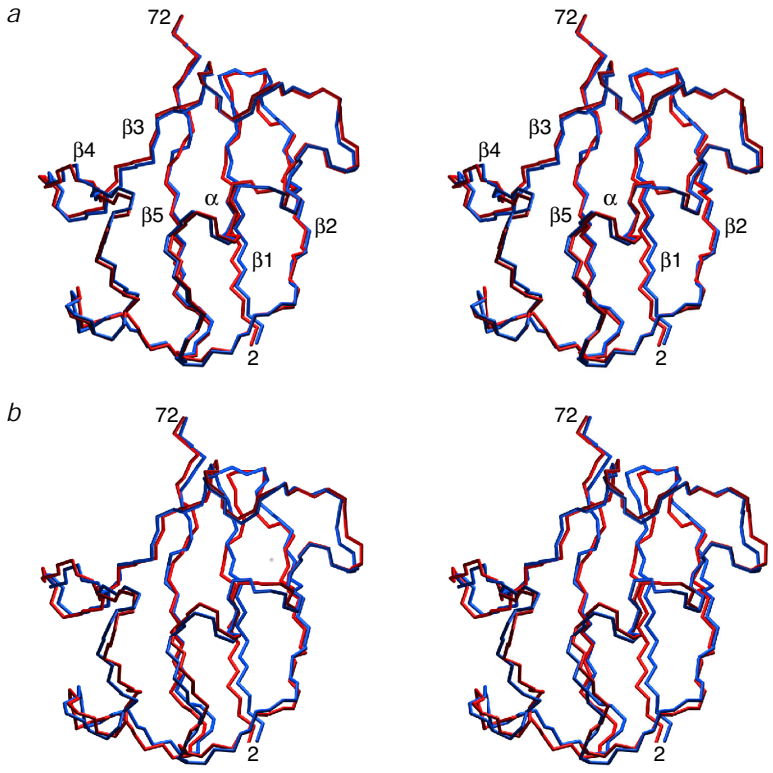

Fig. 6S Stereoviews illustrating (a) two members (shown in red and blue) of a typical ensemble from the 2r set of calculations, and (b) two members (shown in red and blue) of a typical ensemble from the 2pr set of calculations. The structures have been optimally translated relative to one another but no best-fit rotation has been carried out.